eLIFE
elifesciences.org

RESEARCH ARTICLE

Figures and figure supplements

A vitamin-B2-sensing mechanism that regulates gut protease activity to impact animal's food behavior and growth

Bin Qi *et al*

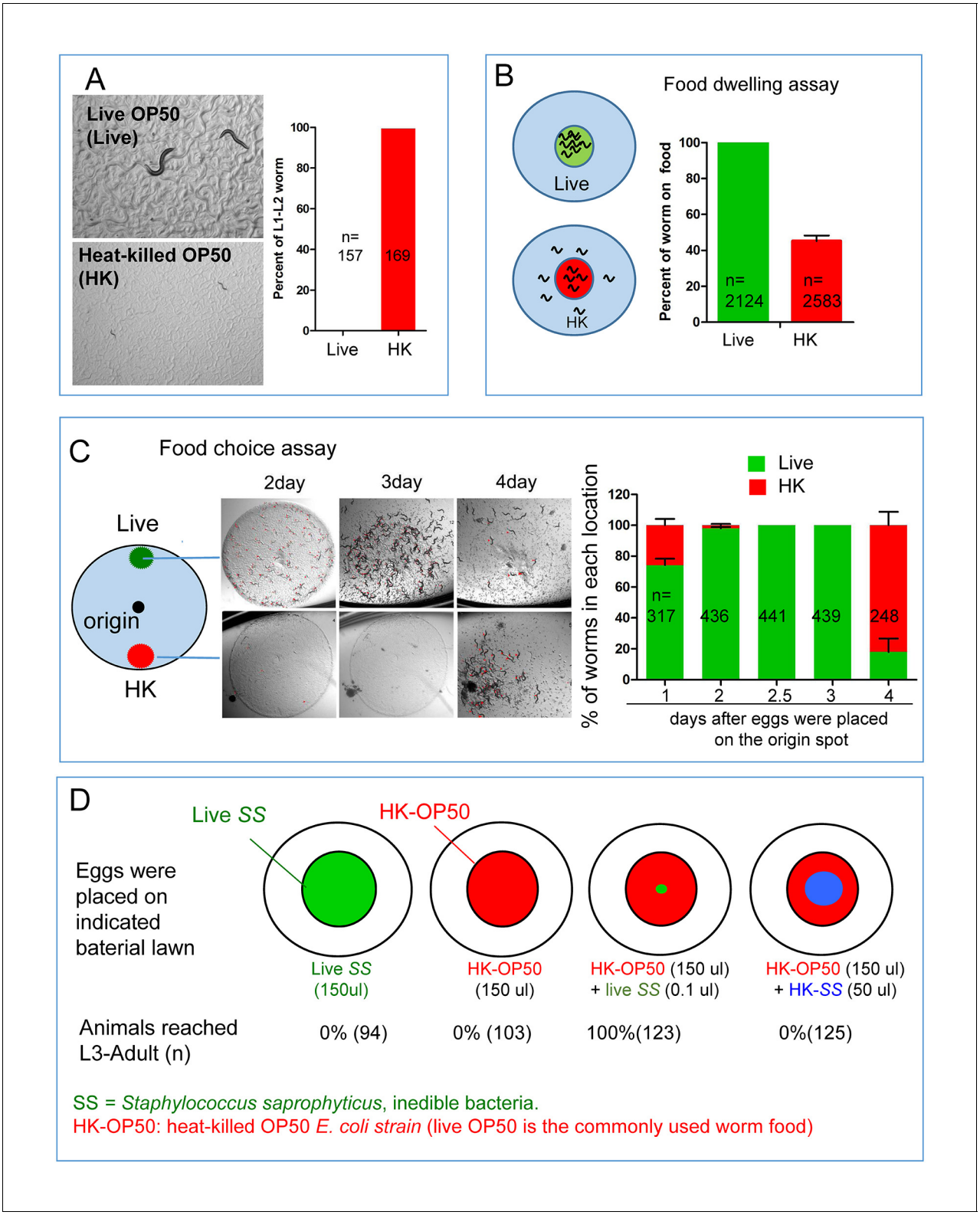

Figure 1. *C. elegans* do not eat heat-killed bacteria without interacting with live bacteria. (**A**) Microscope images and bar graph showing that worms fed heat-killed OP50 (HK-OP50 or HK) arrested at L1-L2 stage three days after hatching. (**B**) Schematic drawing and quantitative data of the food dwelling assay. Circles indicate the food spot for live (green) and HK-OP50 (red) bacteria, respectively. The animals were scored 24 hr after L1 worms were placed on the food spot. Data are represented as mean ±SD. (**C**) Schematic drawing, microscopic images and quantitative data of the food choice assay. Eggs were place in the center spot (origin). Live (green) and heat-killed (red) bacteria were placed on opposite sides of the plate. The

Figure 1 continued on next page

Figure 1 continued

percentage of worms on each spot was calculated at the indicated time. Worms moved to heat-killed bacteria and consumed it after 4 days when live food was totally consumed. Data are represented as mean ±SEM. (**D**) An assay for the effect of a small amount of live, non-edible bacteria on the growth of animals fed heat-killed bacteria. The colored diagrams show the feeding conditions. Percentage of animals that grew to L3-adult stages is indicated below each diagram. The combination of HK-OP50 and small amount live SS, neither of which alone can support growth, could support food uptake and growth. The control (4th column) suggests that only live SS can promote worms to consume HK-OP50. For bar graphs, number of worms scored is indicated in each bar. All data are representative of at least three independent experiments.

DOI: 10.7554/eLife.26243.003

The following source data is available for figure 1:

Source data 1. Numerical data of ***Figure 1A–1D*** and ***Figure 1—figure supplement 1C***.

DOI: 10.7554/eLife.26243.004

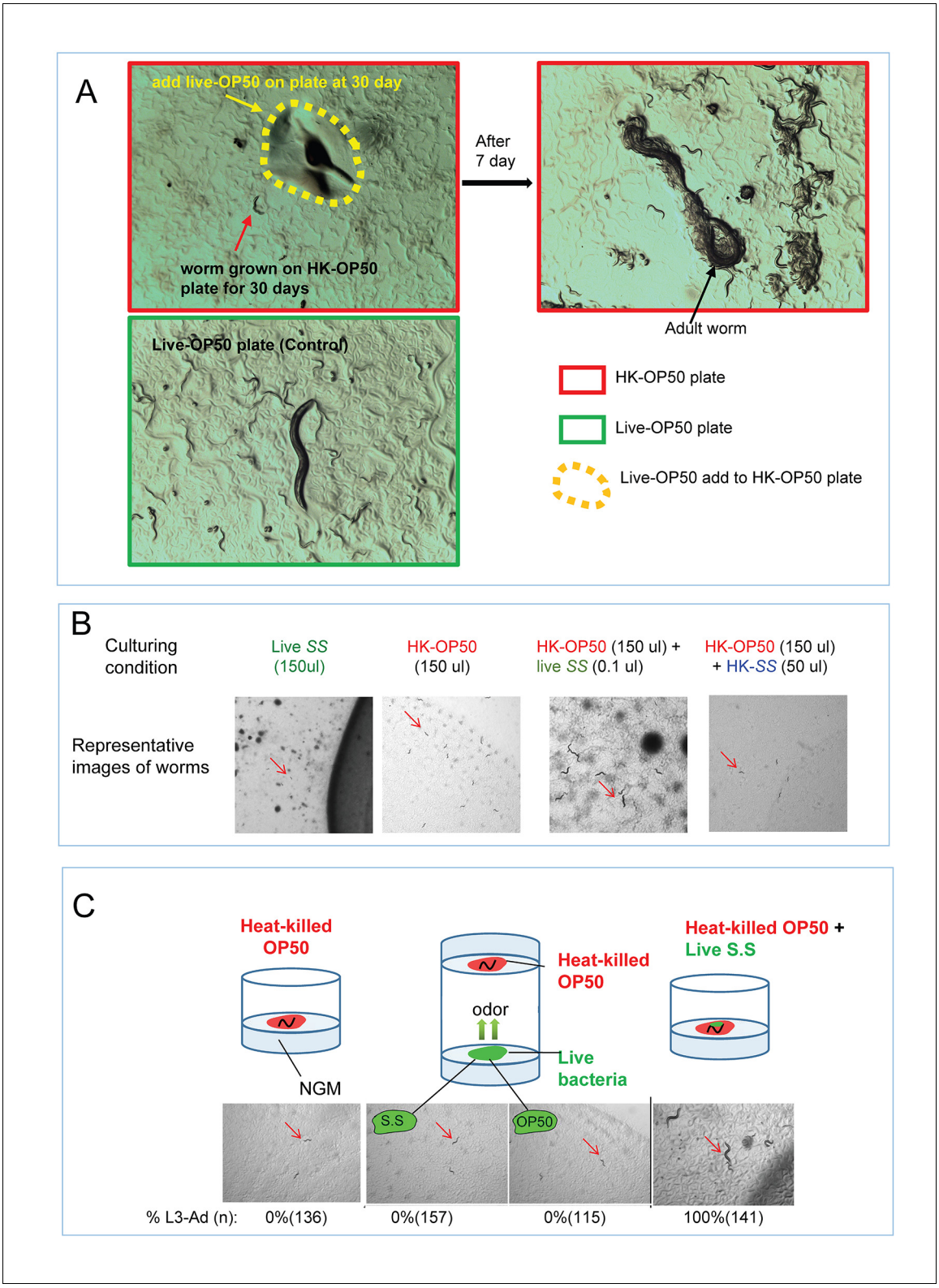

Figure 1—figure supplement 1. Impact of interaction with live bacteria on the ability of *C. elegans* to consume heat-killed bacteria. (**A**) Worms on heat-killed OP50 (growth for 30 days) can be recovered once they eat live OP50. Once live-OP50 (yellow arrow and dotted line) was added to worms (red arrow) grown on HK-OP50 plate for 30 days, they recovered to adults with viable progeny. This result suggests that nutrient deficiency in HK-OP50 induced a protective response from the worms similar to starvation response. (**B**) Representative images of animals in the assay described in ***Figure 1D***. Only under the HK-OP50+ live SS condition, worms were able to consume all heat-killed bacteria and grow. (**C**) Cartoon illustrations, microscopic

Figure 1—figure supplement 1 continued on next page

Figure 1—figure supplement 1 continued

images and quantitative data showing that live bacteria do not influence the usability of heat-killed bacteria through odorants. In the middle cartoon, two petri dishes are stacked with top (opening) facing each other so that the worms/food on the agar pads are exposed to common air space, >100 worms were scored for each testing condition. *S.S.= Staphylococcus saprophyticus*..

DOI: 10.7554/eLife.26243.005

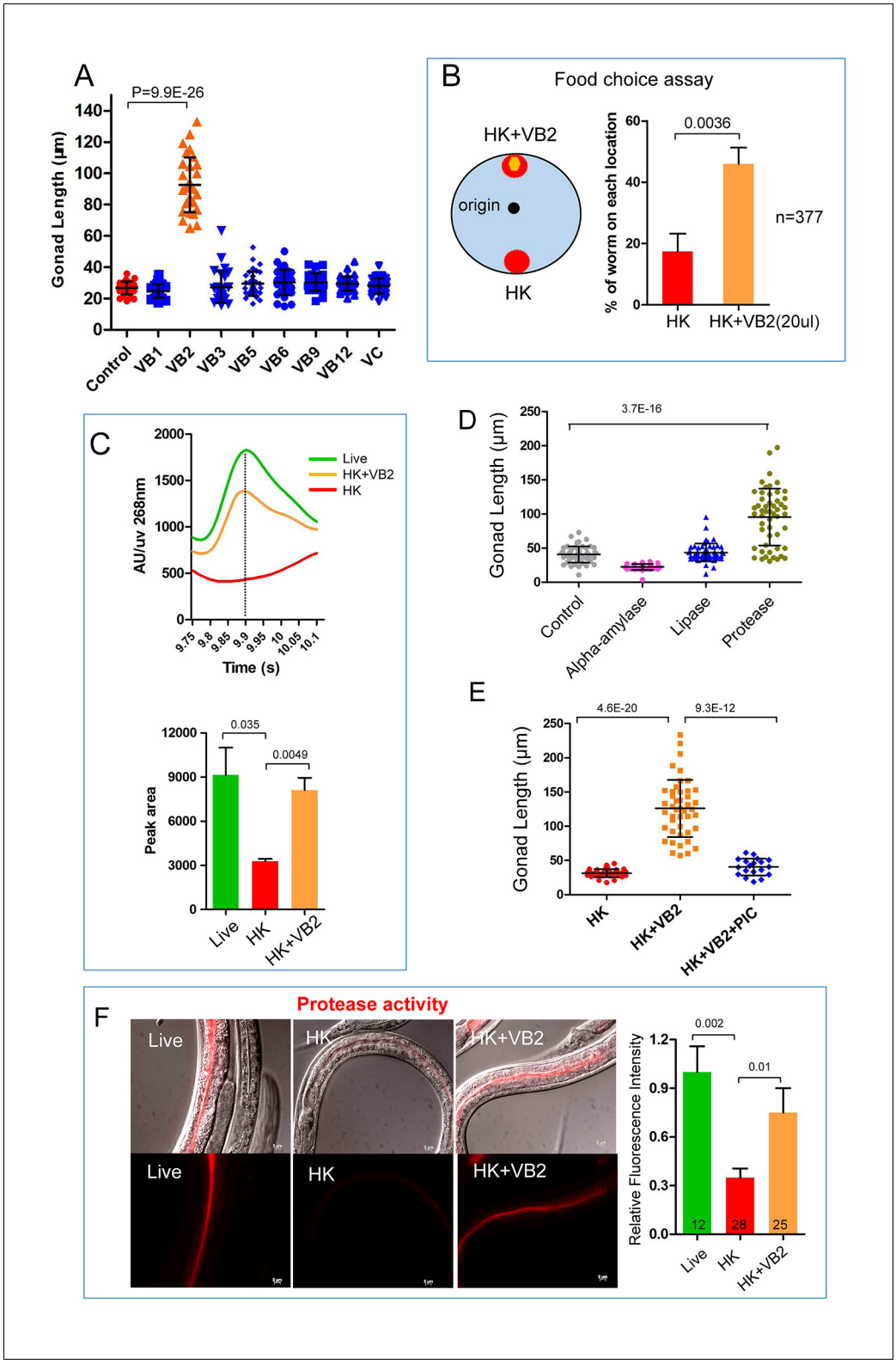

Figure 2. Vitamin B2 (VB2) supplementation increases the usage of heat-killed bacteria and promotes intestinal protease activity. (**A**) Scatter plot of gonad length of worms fed heat-killed OP50 supplemented with indicated vitamins scored at Day 7. > 28 worms were scored for each sample. Representative images are shown in ***Figure 2—figure supplement 1A***. Data are represented as mean ±SD. (**B**) Food-choice assay to test the effect of VB2 supplementation on animal dwelling behavior. The worms were scored for the ratio between the two

Figure 2 continued on next page

Figure 2 continued

locations at 3 day. Data are represented as mean ±SD. (**C**) HPLC-UV analysis of VB2 extracted from worms fed live, HK-OP50 and HK-OP50+VB2 supplementation. The bar graph represents the area counts of VB2 UV absorption peaks (identified by Analyst software), the mean ±SEM of three independent experiments. A graph for VB2 standard from HPLC-UV analysis is shown in ***Figure 2—figure supplement 2B***. (**D**) Scatter plot showing the effect of treating HK-OP50 with indicated enzymes, on larval growth (by measuring gonad length). Only protease treatment significantly promoted growth. The number of worms scored was 52, 37, 52 and 52, respectively. Data are represented as mean ±SD. (**E**) Scatter plot showing the effect of a protease inhibitor cocktail (PIC) on the growth of larvae fed HK-OP50 supplemented with VB2. The number of worms scored was 32, 44 and 18, respectively. Data are represented as mean ±SD. (**F**) Fluorescence images and bar graph showing the impact of heat-killed bacteria and VB2 supplementation on in vivo protease activity in the intestinal tract by the EnzChek protease assay (***Hama et al., 2009***). L2 stage worms were incubated with quenched BODIPY TR-X casein for 3 hr before imaging. Data are represented as mean ±SEM. p-Values were calculated by T-test and $p<0.05$ was considered a significant difference. For bar graphs, number of worms scored is indicated in each bar. All data are representative of at least three independent experiments.

DOI: 10.7554/eLife.26243.006

The following source data is available for figure 2:

Source data 1. Numerical data of ***Figure 2A–2F*** and ***Figure 2—figure supplement 2A, D and E***.

DOI: 10.7554/eLife.26243.007

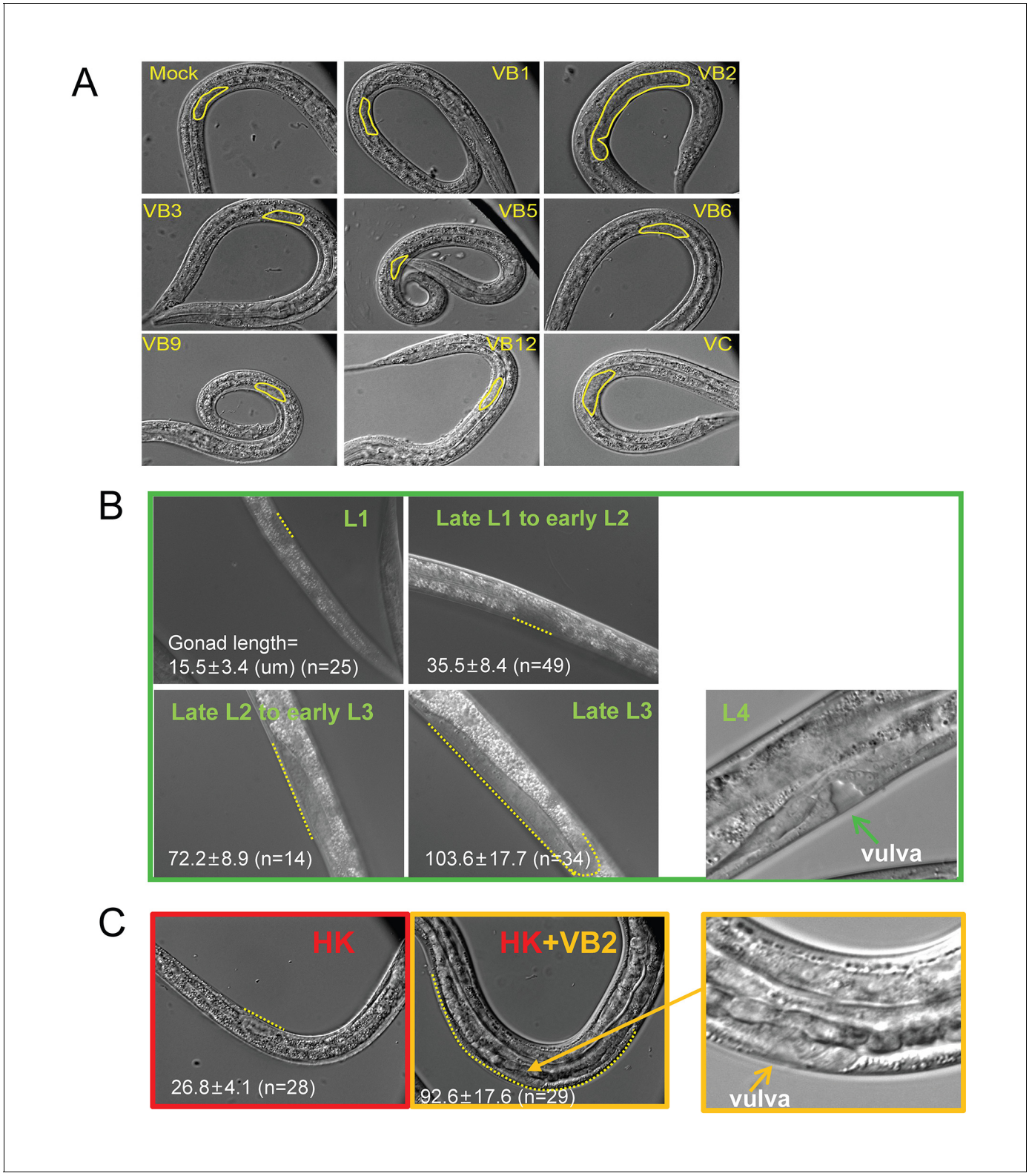

Figure 2—figure supplement 1. Gonad length of worms under different conditions. Under heat-killed bacteria feeding conditions, animals were very unhealthy so that stage progression may not correlate with growth well. Larval growth in this paper as indicated by increase in gonad length. (**A**) Microscopic images of larvae fed HK-OP50 with various vitamin supplements. Gonad length of each worm was measured using ImageJ at Day 7, to evaluate progression of larval growth, which reflects the consumption of the food. The statistical data are shown in the scatter plot in ***Figure 2A***. (**B**) Gonad length (dotted line) of wild-type worms fed live OP50 in different developmental stages, and the vulval morphology (green arrow) of L4 worms.

Figure 2—figure supplement 1 continued on next page

Figure 2—figure supplement 1 continued

(**C**) Gonad length of wild-type worms fed HK-OP50 or HK+VB2 food. If purely based on gonad length (dotted line), worms fed HK food would be at about late L1 to early L2, worms fed HK+VB2 food would be at about late L2 to late L3 stages, comparing to well-fed worms in (**B**). However, the vulval morphology (yellow arrow) of some worms fed HK+VB2 food appeared to reach L4 stage.

DOI: 10.7554/eLife.26243.008

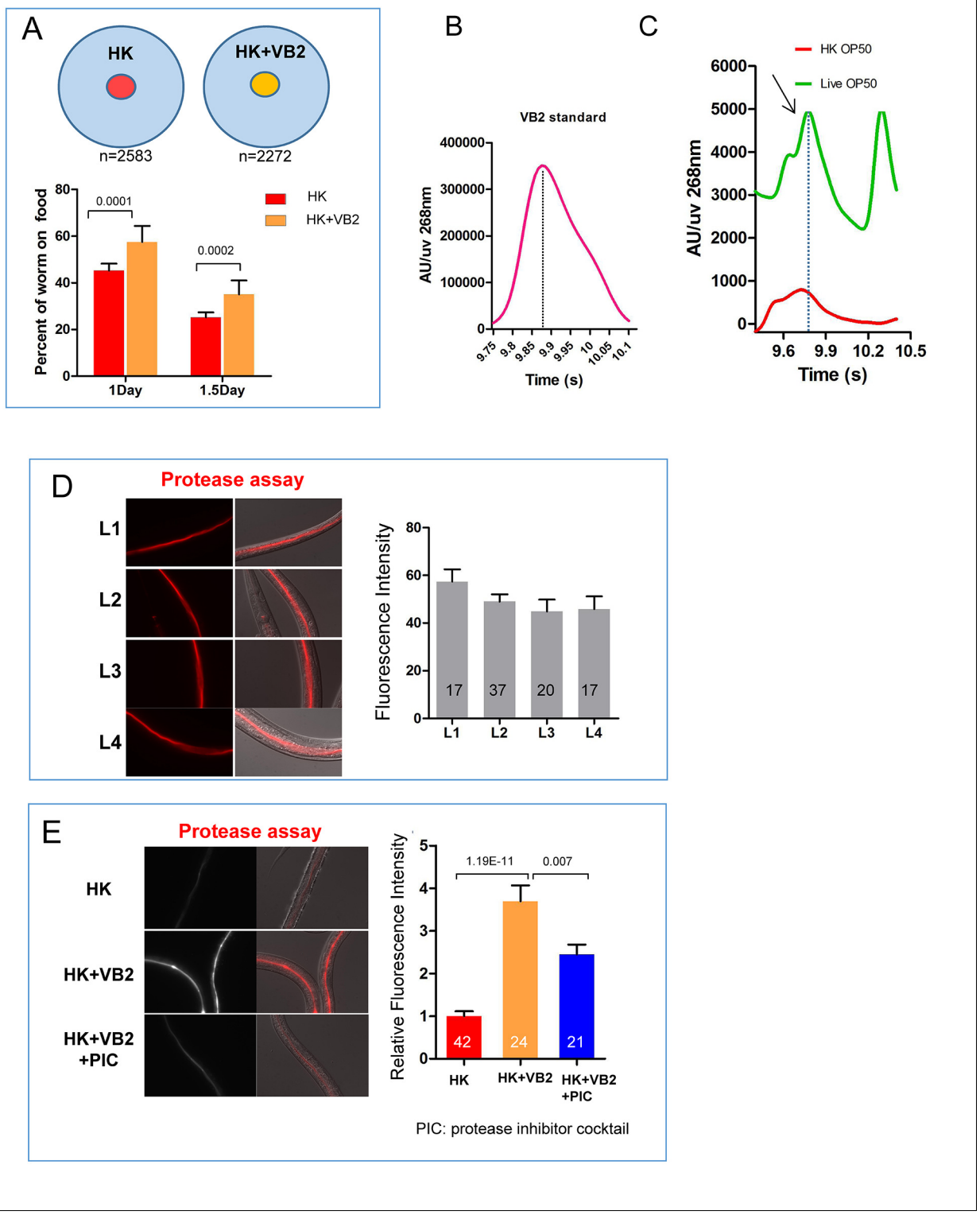

Figure 2—figure supplement 2. Impact of vitamin B2 supplementation on the ability of *C. elegans* to consume heat-killed bacteria. (**A**) Cartoon drawing and quantitative data of the food dwelling assay showing the impact of VB2 supplementation on this behavior. Yellow and red filled circles in the cartoon indicate the spots of HK-OP50 (HK) +/− VB2 supplement, respectively. L1 worms were placed on the food spot and scored for the percent that stayed within the spot after 24 hr. n=number of worms scored. Data are represented as mean ±SD. (**B**) Chromatograph from HPLC-UV analysis of the VB2 standard for the analysis shown in ***Figure 2C***. (**C**) HPLC-UV analysis of VB2 extracted from live and heat-killed OP50. Arrow and dotted line

Figure 2—figure supplement 2 continued on next page

Figure 2—figure supplement 2 continued

indicate the peak of VB2. (**D**) BODIPY-labeled protease activity in the intestinal tract of worms fed live OP50 at four different larval stages. Fluorescence intensity was measured by ImageJ software. Data are represented as mean ±SEM. (**E**) Effects of VB2 supplementation and treatment of protease inhibitor on in vivo protease activity in worms fed HK-OP50. Data are represented as mean ±SEM. p Values were calculated by T-test. and $p<0.05$ was considered a significant difference.

DOI: 10.7554/eLife.26243.009

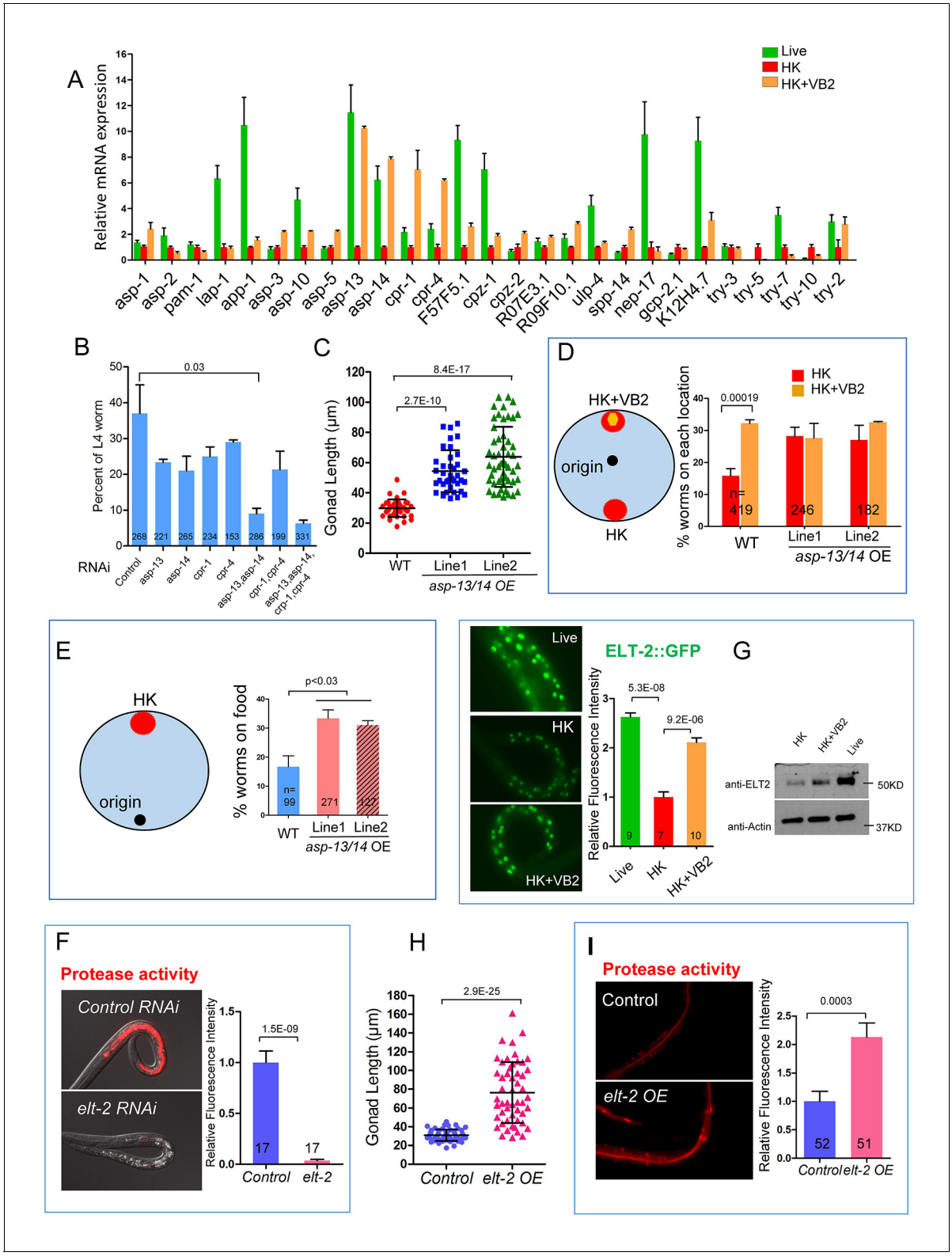

Figure 3. Proteases ASP-13 and ASP-14 and GATA factor ELT-2 play critical roles in VB2-promoted food usability and animal growth. (**A**) Results of qRT-PCR analysis showing the expression of indicated protease genes in wild-type worms fed indicated food. Data are represented as mean ±SEM. (**B**) Impact of RNAi of indicated genes on larval growth when fed HK-OP50+VB2 supplementation. Worms with both *asp-13* and *asp-14* knocked down displayed strongest effect. Data are represented as mean ±SEM. (**C**) Scatter plot showing the impact of over-expression of the two protease genes behind the *rpl-28* promoter, measured by gonad length of larvae fed HK-OP50 at Day 7. n = 41, 39 and 52, respectively. Data are represented as mean

Figure 3 continued on next page

Figure 3 continued

±SD. (**D and E**) Cartoon diagram and data from food choice (**D**) and food seeking (**E**) assays showing that overexpression of *asp-13* and *asp-14* (*asp-13/14* OE) eliminated the discrimination against HK-OP50 over HK-OP50+VB2 (**D**) and improved affinity of worms towards HK-OP50 (**E**). Data from two different overexpression lines are shown. Data are represented as mean ±SEM. (**F**) Fluorescence images and bar graph showing protease activity in the intestinal tract is dramatically decreased in worms treated with *elt-2(RNAi)*. Data are represented as mean ±SEM. (**G**) Fluorescence images (integrated translational ELT-2::GFP reporter strain) and Western blot (wild-type strain) showing that the ELT-2 expression is prominently decreased in worms fed HK-OP50 compared to that in worms fed live OP50, and the expression is largely recovered by VB2 supplementation. Data are represented as mean ±SEM. (**H**) Scatter plot showing larval growth measured by gonad length of worms fed heat-killed OP50 is increased by an *elt-2* over-expression transgene (OE) at Day 7. n = 52 for each condition. Data are represented as mean ±SD. (**I**) Fluorescence images and bar graph showing that the protease activity is increased in *elt-2* overexpression (*elt-2 OE*) worms fed HK-OP50. p-Values were calculated by T-test. For bar graphs, number of worms scored is indicated in each bar. Data are represented as mean ±SEM. p-Values were calculated by T-test and $p<0.05$ was considered a significant difference. For bar graphs, number of worms scored is indicated in each bar. All data are representative of at least three independent experiments.

DOI: 10.7554/eLife.26243.010

The following source data is available for figure 3:

Source data 1. Numerical data of ***Figures 3B–2I*** and ***Figure 3—figure supplements 1A, B, 2A, C and E***.

DOI: 10.7554/eLife.26243.011

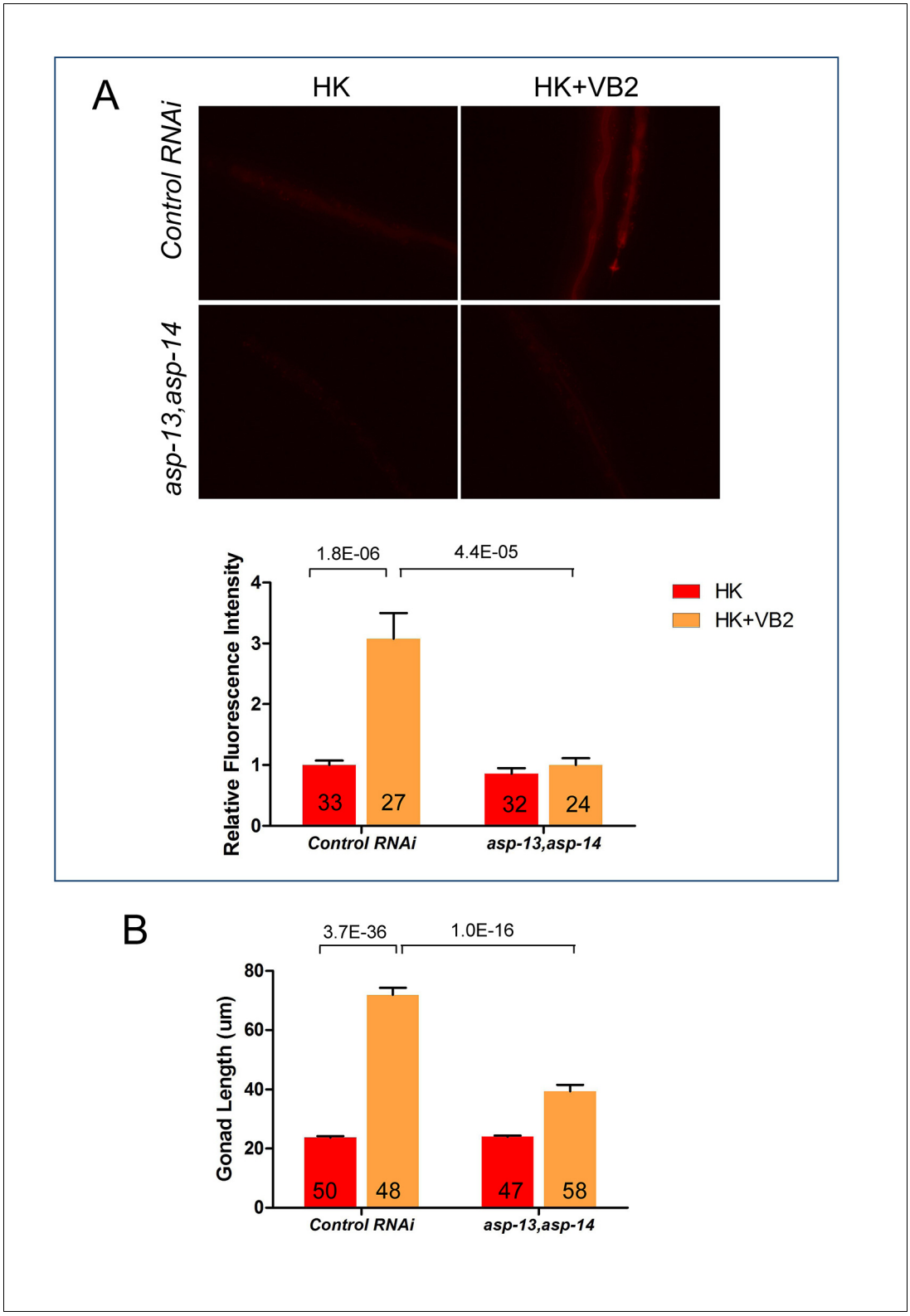

Figure 3—figure supplement 1. VB2 supplementation-induced increase in protease activity and growth rescue in worms fed HK-food depend on intestinal expression of ASP-13 and ASP-14. Intestine-specific RNAi of *asp-13* and *asp-14* blocked the increases in protease activity (**A**) and gonad length (**B**) caused by VB2 supplementation on worms fed HK. Data are represented as mean ±SEM.

DOI: 10.7554/eLife.26243.012

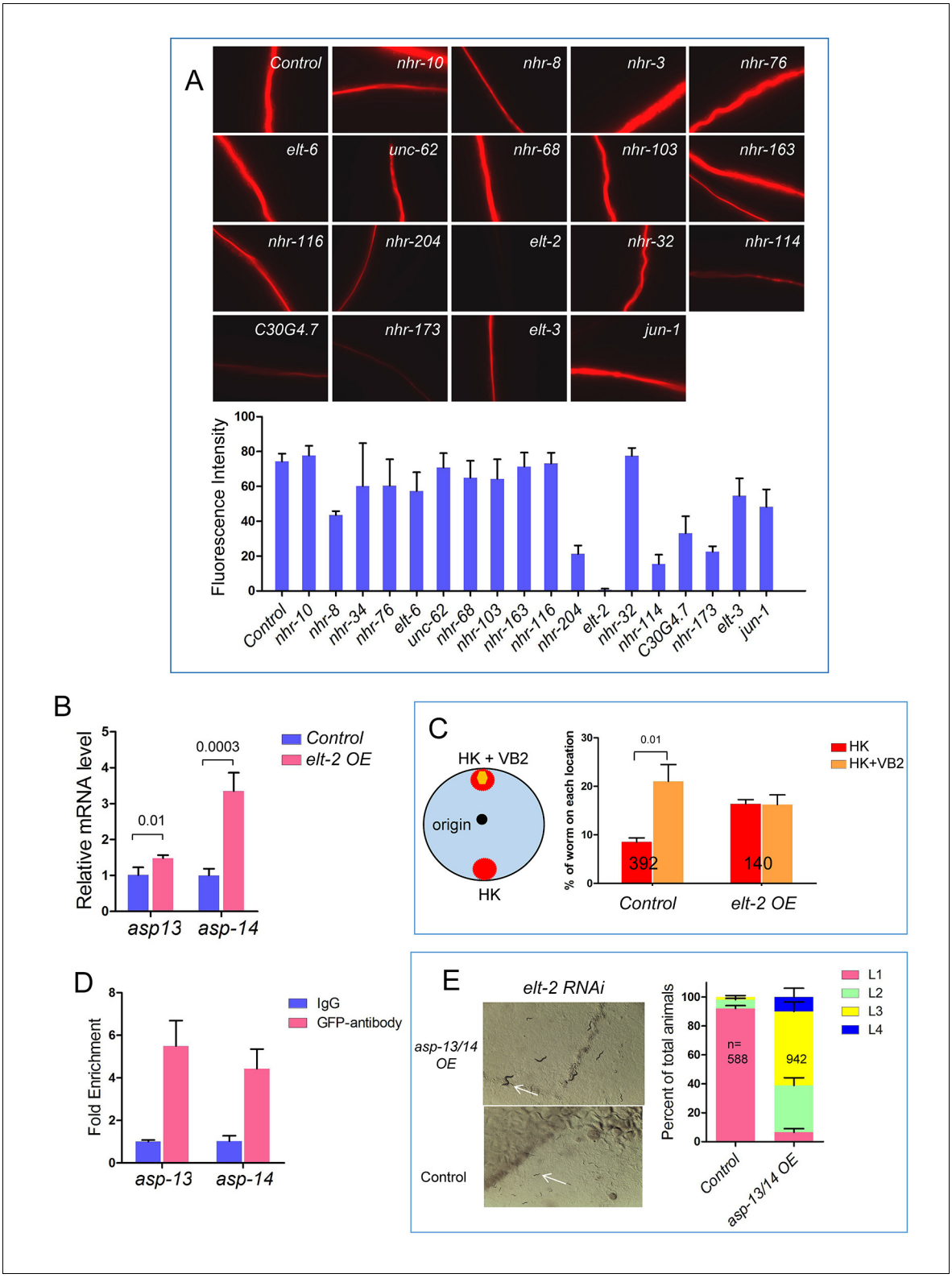

Figure 3—figure supplement 2. Roles of protease ASP-13 and ASP-14, and GATA factor ELT-2 in VB2-induced food uptake and growth of worms fed heat-killed bacteria. (**A**) Representative images and quantitative data from the protease assay on worms treated with RNAi of indicated genes in a screen for transcription factors required for intestinal protease activity. Synchronized L1s were transferred onto plates seeded with individual RNAi bacterial clones. The protease activity in the intestinal tract of L1-L2 worms of the next generation was measured. *elt-2*(RNAi) displayed the most dramatic decrease (also see ***Figure 2D***). Fluorescence intensity was measured by ImageJ software. Data are represented as mean ±SEM. (**B**) qRT-PCR

Figure 3—figure supplement 2 continued on next page

Figure 3—figure supplement 2 continued

data showing that mRNA of *asp-13* and *asp-14* are increased in *elt-2* overexpression (*elt-2 OE*) worms fed HK-OP50. Data are represented as mean ±SD. (**C**) Results of a food choice assay showing that over expression of *elt-2* (*elt-2 OE*) eliminated the discrimination of worms against HK-OP50 over HK-OP50+VB2. Data are represented as mean ±SEM. (**D**) ChIP-qPCR data showing enrichment of ELT-2 binding to *asp-13* and *asp-14* promoters. Samples from a strain expressing an ELT-2::GFP fusion transgene were subject to immunoprecipitation using either control IgG or anti-GFP antibody. Data are represented as mean ±SD. This result is consistent with the data from a recent ChIP-seq analysis suggested that *asp-13* and *asp-14* are likely direct targets of ELT-2 (***Mann et al., 2016***). (**E**) Microscopic images and bar graph showing that overexpression of *asp-13* and *asp-14* significantly suppressed the larval arrest phenotype of *elt-2*(RNAi). Arrowheads point to two representative animals to indicate the size difference under the two conditions. Data are represented as mean ±SD. Since over-expressing *asp-13* and *asp-14* behind the *rpl-28* promoter is expected to elude regulation by ELT-2, this result supports that down-regulating *asp-13* and *asp-14* by a low ELT-2 level critically contributes to the poor food usage in worms fed HK-OP50. All data are representative of at least three independent experiments.

DOI: 10.7554/eLife.26243.013

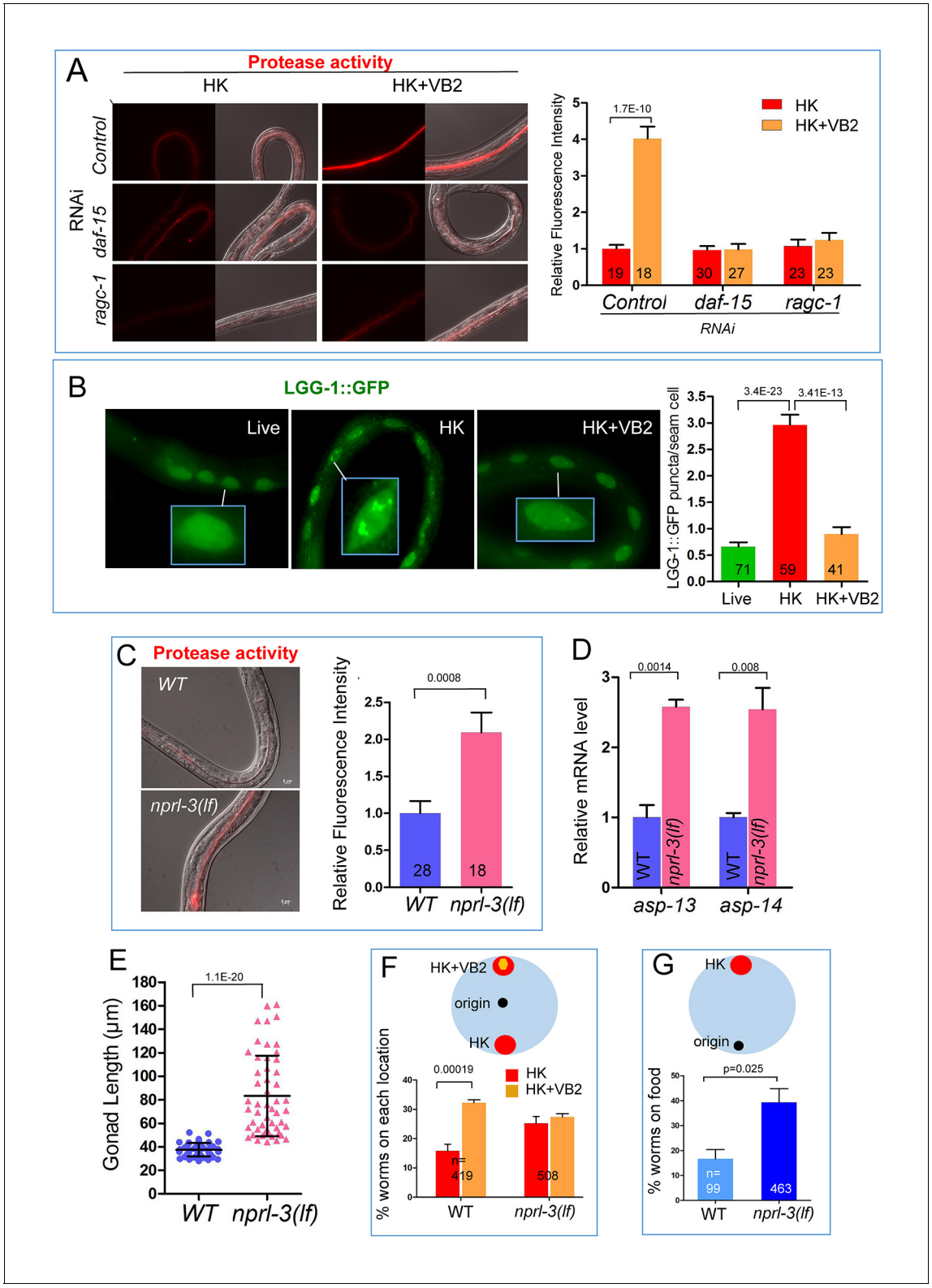

Figure 4. TORC1 mediates the impact of VB2 on the expression of digest enzymes and food usage. (**A**) Fluorescence images and bar graph showing that VB2-induced increase in protease activity in the digestive tract depends on TORC1 function. Data are represented as mean ±SEM. (**B**) Fluorescence images and bar graph showing that autophagy activity (measured by the intensity of LGG-1::GFP puncta in seam cells) increases in worms fed HK-OP50, compared to worms fed live OP50, and the increase is eliminated by VB2 supplementation. The inset image in each panel shows magnified area indicated by the white bar. ***Figure 4—figure supplement 2A and B*** show data supporting that LGG-1 puncta is repressed by TORC1 activity,

Figure 4 continued on next page

Figure 4 continued

consistent with known negative regulation of autophagy by TORC1 (***Robida-Stubbs et al., 2012***). Data are represented as mean ±SEM. (**C**) Fluorescence images and bar graph showing that protease activity is increased in an *nprl-3(lf)* mutant fed HK-OP50. *nprl-3* negatively regulates TORC1 (***Zhu et al., 2013***). Data are represented as mean ±SEM. (**D**) qRT-PCR analysis showing that mRNA of *asp-13* and *asp-14* were increased in *nprl-3(lf)* mutant fed HK-OP50. Data are represented as mean ±SEM. (**E**) Scatter plot showing that larval growth is increased in the *nprl-3(lf)* mutant worms fed HK-OP50 at Day 7. n = 52 for each condition. Data are represented as mean ±SD. (**F and G**) Result from food choice (**F**) and food-seeking (**G**) assays showing that *nprl-3(lf)*, which hyperactivates TORC1, eliminated the discrimination against HK-OP50 over HK-OP50+VB2 (**F**) and improved affinity of worms toward HK-OP50 (**G**). The wild-type data are the same as that in ***Figure 3D and E***, as the data for both pairs of figures were generated from the same set of experiments. Data are represented as mean ±SEM. p-Values were calculated by T-test and $p<0.05$ was considered a significant difference. For bar graphs, number of worms scored is indicated in each bar. All data are representative of at least three independent experiments.

DOI: 10.7554/eLife.26243.014

The following source data is available for figure 4:

Source data 1. Numerical data of ***Figure 4A–4C and E–G*** and ***Figure 4—figure supplements 1***, ***2A, B, D, F and G***.

DOI: 10.7554/eLife.26243.015

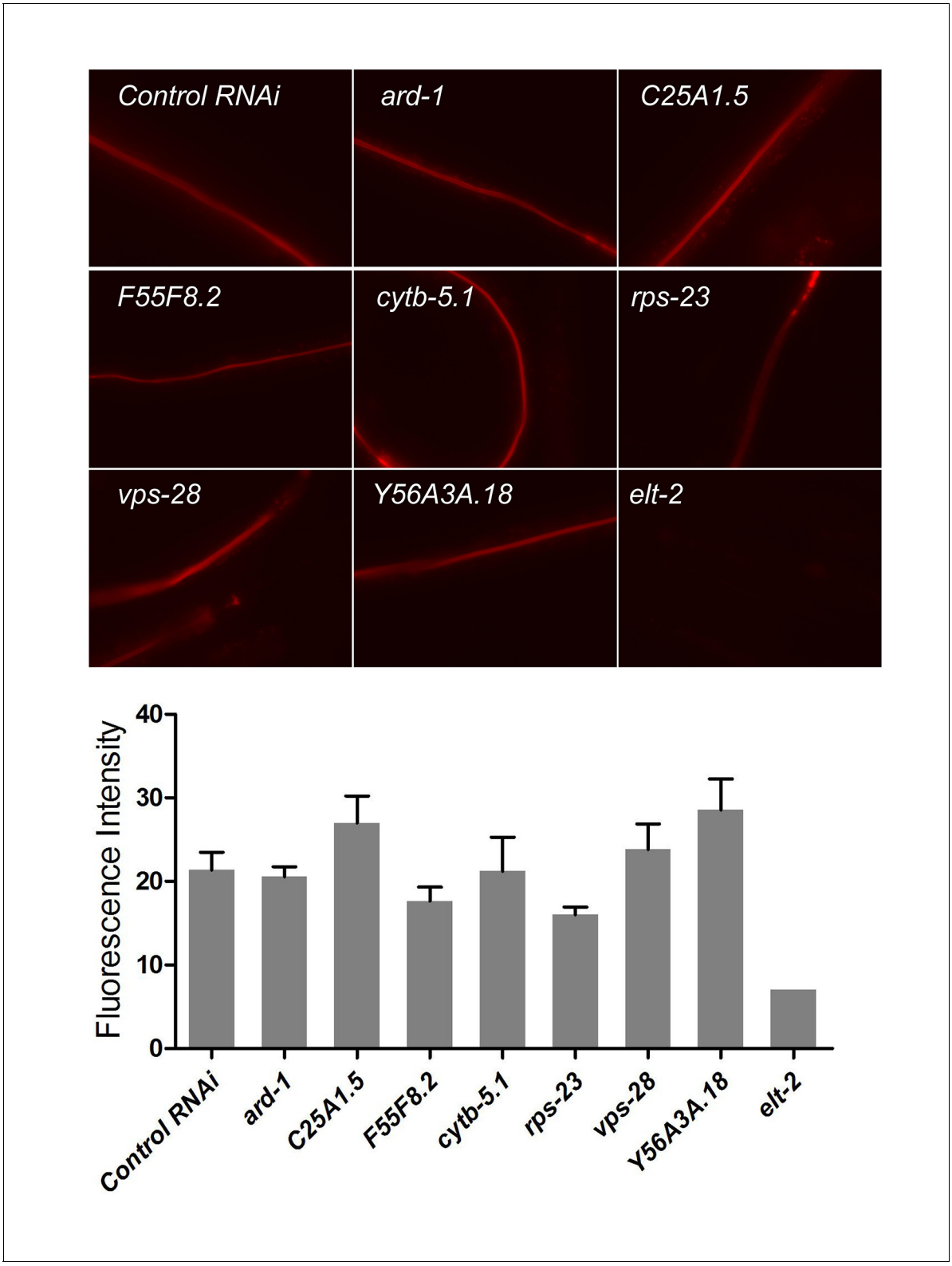

Figure 4—figure supplement 1. Protease activity of several arrested larvae (RNAi treatment), *elt-2* RNAi as positive control. Protease activity is not all reduced in arrested larvae, which indicate that lower TORC1 activity on protease activity (***Figure 4A***) is unlikely to be from generally slowing or arresting development.

DOI: 10.7554/eLife.26243.016

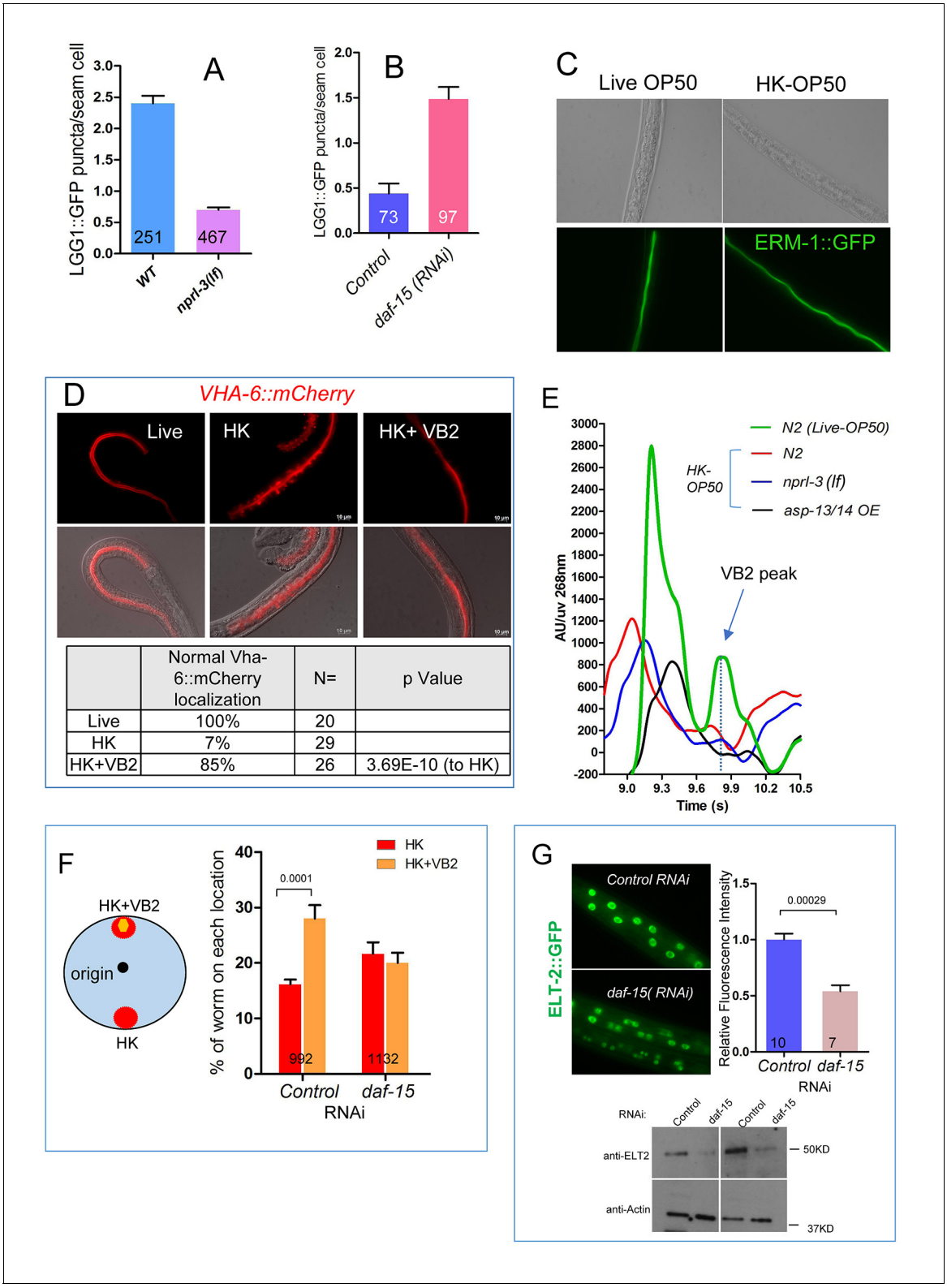

	Normal Vha-6::mCherry localization	N=	p Value
Live	100%	20	
HK	7%	29	
HK+VB2	85%	26	3.69E-10 (to HK)

Figure 4—figure supplement 2. LGG-1::GFP as a marker for activity downstream of TORC1 and the impact of food source on apical membrane polarity and VHA-6 localization in the intestine of *C. elegans*. (**A**) Bar graph showing that the high level of autophagy activity (measured by the number of LGG-1::GFP puncta in seam cells) in worms fed HK-OP50 (see ***Figure 4B***) is suppressed by an *nprl-3(lf)* mutation that hyperactivates TORC1 (***Zhu et al., 2013***). Data are represented as mean ±SEM. (**B**) RNAi knockdown of *daf-15*, which reduces TORC1 activity, caused a drastic increase in autophagy activity in young wild type larvae. Data are represented as mean ±SEM. (**C**) Fluorescence images showing that apical localization of ERM-1::GFP, a

Figure 4—figure supplement 2 continued on next page

Figure 4—figure supplement 2 continued

marker for the integrity of apical membrane polarity (***Zhang et al., 2011***; ***Zhu et al., 2015***), in the intestine is not altered in worms fed heat-killed bacteria. The results suggest that the apical membrane polarity of the intestine is not defective under the poor feeding condition. (**D**) Fluorescence images and quantitative data showing that localization of a VHA-6::mCherry fusion protein is disorganized at the apical membrane of the intestine of worms fed heat-killed bacteria (HK). The defect is significantly suppressed by VB2 supplementation. VHA-6 is a subunit of the vacuolar type H+-ATPase (V-ATPase) that has been indicated to function in TORC1 activation in mammalian cell culture studies (***Zoncu et al., 2011***). VHA-6 and its localization at the apical membrane have been linked to TORC1 activity in response to defects in a lipid biosynthesis pathway in *C. elegans* (***Zhu et al., 2015***). These data are consistent with the proposed reduction of TORC1 activity in worms fed heat-killed bacteria and recovery of TORC1 activity by VB2 supplementation. (**E**) HPLC-UV analysis of VB2 extracted from wild-type worm fed live OP50, or wild-type, *nprl-3(lf)* and *asp-13/14 OE* worms fed HK-OP50. Arrow indicates the peak of VB2. (**F**) Reducing TORC1 activity (*daf-15* RNAi) led to defects in food choice. Data are represented as mean ±SEM. (**G**) Fluorescence images (integrated translational ELT-2::GFP reporter strain) and Western blot (wild-type) showing that *daf-15(RNAi)* caused a decrease in ELT-2 expression in worms fed live OP50. Data are represented as mean ±SEM. p-Values were calculated by T-test. For bar graphs, the number of worms scored is indicated within each bar.

DOI: 10.7554/eLife.26243.017

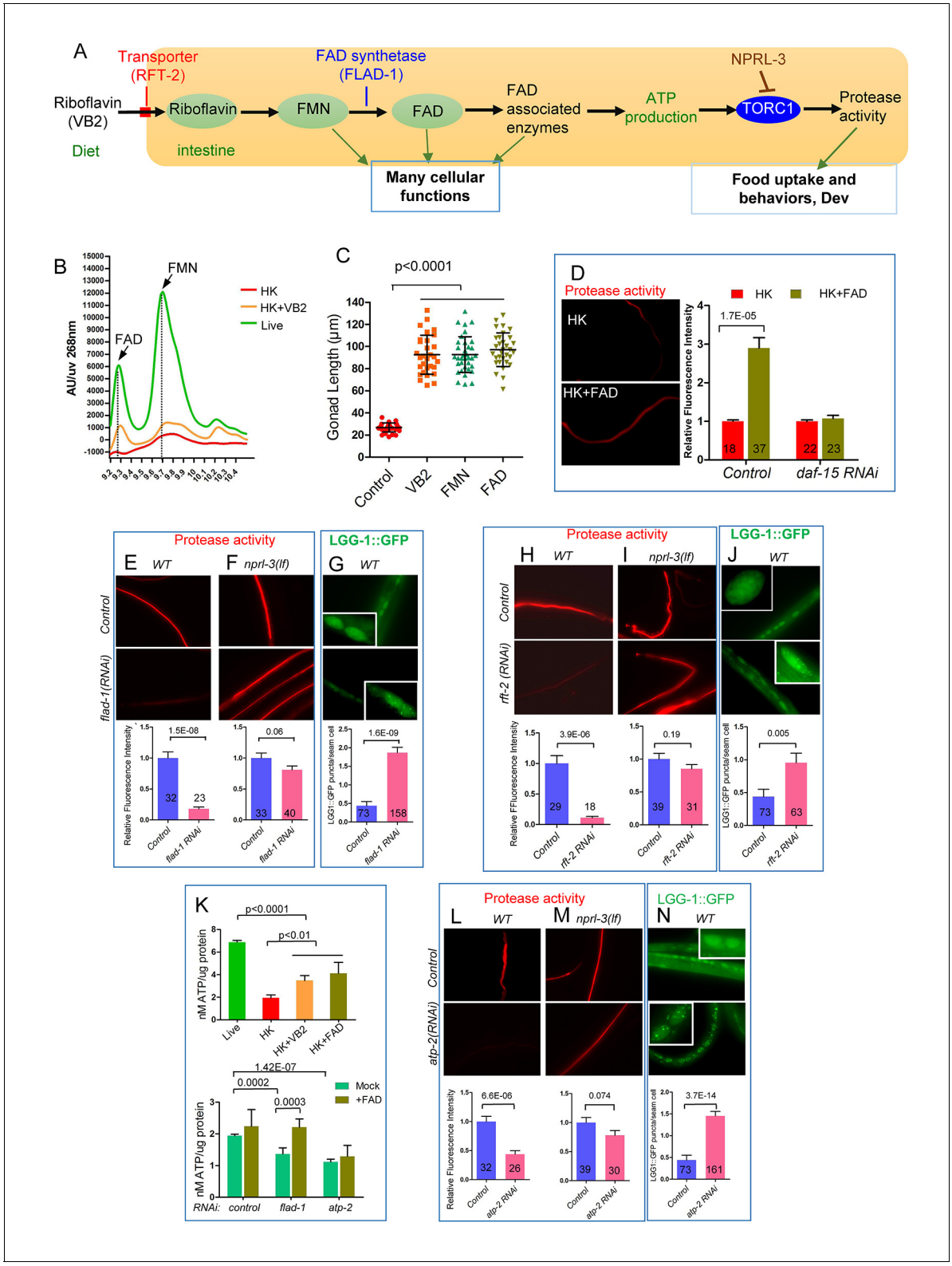

Figure 5. Change in FAD may mediate the effect of VB2 on food usage by worms fed heat-killed bacteria. (**A**) Cartoon diagram to illustrate known functional relationship between VB2 (riboflavin), flavin mononucleotide (FMN) and flavin adenine dinucleotide (FAD), as well as a proposed VB2 sensing pathway in the intestine, based on this study. *RFT-2, expressed in the intestine in C. elegans*, is a homolog of the riboflavin transporter three that is required for VB2 uptake (***Biswas et al., 2013***; ***Gandhimathi et al., 2015***). *FLAD-1* is a FAD synthase that catalyzes the last step of FAD biosynthesis (***Liuzzi et al., 2012***). NPRL-3 represses TORC1 activity (***Zhu et al., 2013***). (**B**) HPLC-UV detection peak of FAD and FMN from worms fed under

Figure 5 continued on next page

Figure 5 continued

indicated conditions. ***Figure 5—figure supplement 1A*** shows the graph of FAD and FMN standards. (**C**) Scatter plot showing that supplementation of FMN or FAD significantly recovered the of wild-type larvae fed HK-OP50. The number of worms scored was 28, 29, 35 and 31, respectively. Data are represented as mean ±SD. (**D**) Fluorescence images and bar graph showing that FAD supplementation elevated the in vivo protease activity in worms fed HK-OP50 and the increase is eliminated by RNAi knockdown of *daf-15/raptor*. Data are represented as mean ±SEM. (**E and F**) Fluorescence images and bar graph showing that RNAi knock down of *flad-1*/FAD synthetase sharply reduced the in vivo protease activity in wild type (**E**). The reduction was suppressed by a *nprl-3(lf)* mutation (**F**) that hyperactivates TORC1. Data are represented as mean ±SEM. (**G**) RNAi knockdown of *flad-1* elevated autophagy activity (LGG-1::GFP puncta) that is known to be repressed by TORC1. Data are represented as mean ±SEM. (**H and I**) Fluorescence images and bar graph showing that RNAi knock down of *rft-2*, encoding a riboflavin transporter (see A), sharply reduced the in vivo protease activity in wild type. The sharp reduction was suppressed by a *nprl-3(lf)* mutation that hyperactivates TORC1. Data are represented as mean ±SEM. (**J**) RNAi reduction of *rft-2* elevated the number of LGG-1::GFP puncta that marks the level of autophagy. The increase in autophagy is consistent with a reduction in TORC1 activity. Data are represented as mean ±SEM. (**K**) Measurement of ATP levels in worms. (top) ATP level is reduced in worms fed HK-OP50 and the reduction is partially suppressed by VB2 or FAD supplementation. (bottom) *flad-1(RNAi)* or *apt-2(RNAi)* caused reduction in ATP level in wild type, and the decrease by *flad-1(RNAi)*, but not by *atp-2(RNAi)*, was overcome by FAD supplement. Data are represented as mean ±SD. (**L and M**) Fluorescence images and bar graph showing that RNAi knock down of *atp-2*/ATP synthetase, significantly reduced the intestinal protease activity in wild type (**L**). The reduction seen was suppressed by an *nprl-3(lf)* mutation (**M**). Data are represented as mean ±SEM. (**N**) RNAi knock down of *atp-2* elevated the autophagy activity (LGG-1::GFP puncta). Data are represented as mean ±SEM. p-Values were calculated by T-test and $p<0.05$ was considered a significant difference. For bar graphs, the number of worms scored is indicated within each bar. All data are representative of at least three independent experiments.

DOI: 10.7554/eLife.26243.018

The following source data is available for figure 5:

Source data 1. Numerical data of ***Figure 5B–5N*** and ***Figure 5—figure supplement 1B***.

DOI: 10.7554/eLife.26243.019

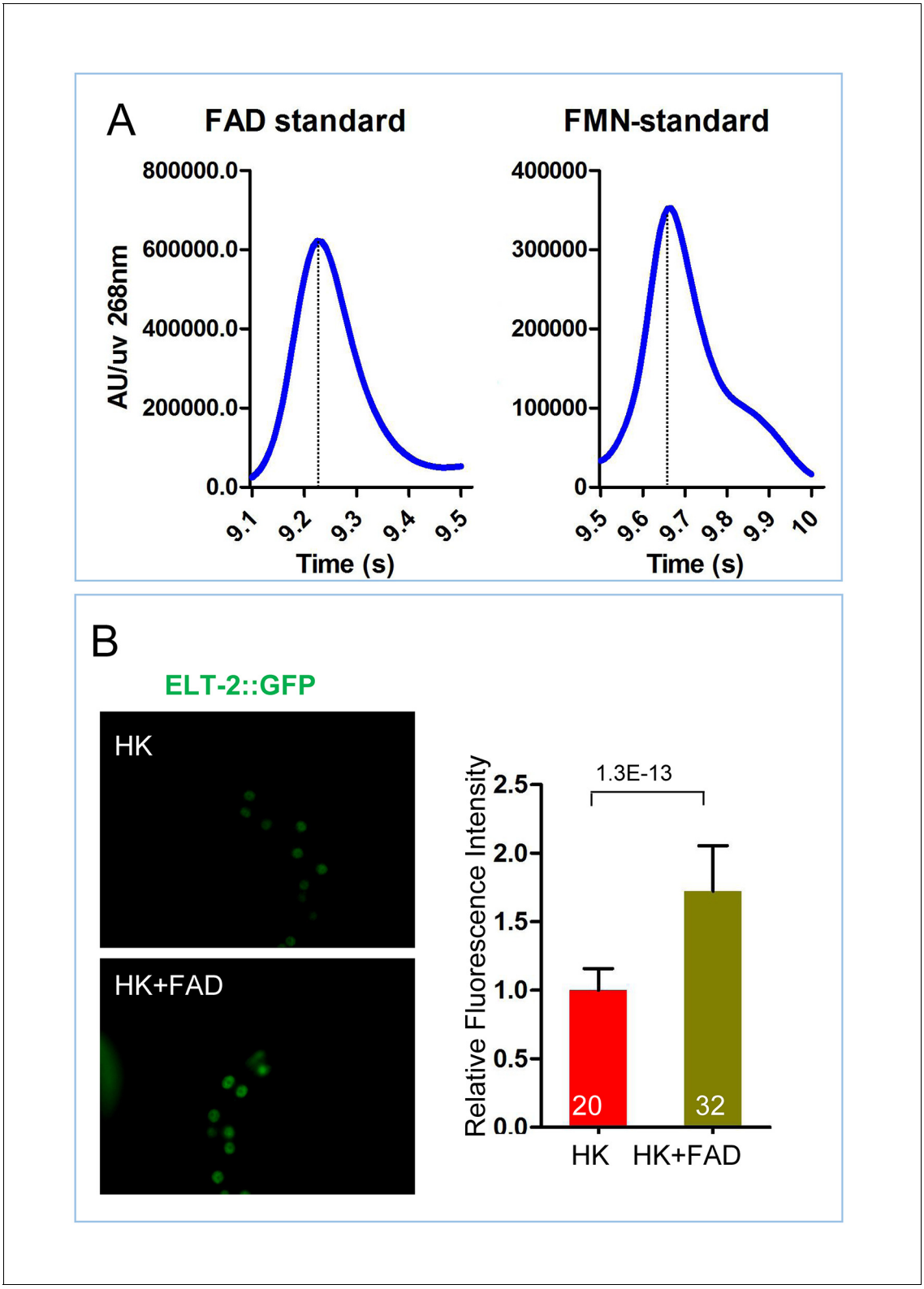

Figure 5—figure supplement 1. Measurement of FAD and FMN standards and role of FAD supplementation on ELT-2 expression. (**A**) HPLC-UV detection peak of FAD and FMN standards, controls for ***Figure 5B***. (**B**) Fluorescence images and bar graph showing that FAD supplementation increases the expression of an ELT-2::GFP reporter in worms fed HK-OP50. Data are represented as mean ±SD.

DOI: 10.7554/eLife.26243.020